



The cholesteryl ester transfer protein (CETP) raises cholesterol levels in the brain

Felix Oestereich^{1,2,3}, Noosha Yousefpour¹, Ethan Yang⁴, Jasmine Phénix^{1,2}, Zari Saadati Nezhad⁴, Albert Nitu^{1,2}, Antonio Vázquez Cobá^{2,3}, Alfredo Ribeiro-da-Silva¹, Pierre Chaurand⁴, and Lisa Marie Munter^{1,2*}

¹Department of Pharmacology and Therapeutics, McGill University, Montreal, Québec, Canada; ²Cell Information Systems Group, Bellini Life Sciences Complex, Montreal, Québec, Canada; ³Integrated Program in Neuroscience, McGill University, Montreal, Québec, Canada; and ⁴Department of Chemistry, Université de Montréal, Montreal, Québec, Canada

Abstract The cholesteryl ester transfer protein (CETP) is a lipid transfer protein responsible for the exchange of cholesteryl esters and triglycerides between lipoproteins. Decreased CETP activity is associated with longevity, cardiovascular health, and maintenance of good cognitive performance. Interestingly, mice lack the CETP-encoding gene and have very low levels of LDL particles compared with humans. Currently, the molecular mechanisms induced because of CETP activity are not clear. To understand how CETP activity affects the brain, we utilized *CETP* transgenic (*CETP*^{Tg}) mice that show elevated LDL levels upon induction of CETP expression through a high-cholesterol diet. *CETP*^{Tg} mice on a high-cholesterol diet showed up to 22% higher cholesterol levels in the brain. Using a microarray on mostly astrocyte-derived mRNA, we found that this cholesterol increase is likely not because of elevated de novo synthesis of cholesterol. However, cholesterol efflux is decreased in *CETP*^{Tg} mice along with an upregulation of the complement factor C1Q, which plays a role in neuronal cholesterol clearance. Our data suggest that CETP activity affects brain health through modulating cholesterol distribution and clearance. Therefore, we propose that *CETP*^{Tg} mice constitute a valuable research tool to investigate the impact of cholesterol metabolism on brain function.

Supplementary key words Alzheimer's disease • CETP transgenic mice • LDL • 24S-hydroxycholesterol • mass spectrometry • microarray • brain lipids • complement system • C1Q • TREM2

Cholesterol is a major constituent of biomembranes and precursor for various hormones. In most tissues, the cholesterol concentration is about 2 mg/g tissue; however, it reaches 15–20 mg/g in the tissue of the CNS (1). Thus, the brain contains 25% of the total body cholesterol, suggesting a special need of the brain for cholesterol (2). In the blood, dietary cholesterol is

transported by VLDL or LDL particles that are secreted by the liver to deliver cholesterol to extrahepatic tissues (3). Reverse cholesterol transport from the periphery back to the liver occurs via HDL particles (4). However, the brain seems to be excluded from these distribution cycles since neither VLDL particles nor LDL particles cross the blood-brain barrier, leading to the conclusion that cholesterol metabolism in the brain is separated from that of the periphery (2, 5–7). In the CNS, astrocytes are the cell types primarily involved in lipid synthesis and secrete HDL-like lipoprotein particles that contain predominantly apolipoprotein E (APOE) as the apolipoprotein (8). Such particles are taken up by neurons through members of the LDL-receptor (LDLR) family that recognize APOE including the LDLR-related protein 1 (LRP1) (9).

The cholesteryl ester transfer protein (CETP) is a lipid transfer protein that facilitates the exchange of cholesteryl esters in HDL for triglyceride in VLDL and LDL (10, 11). The net result of this transfer activity is increased cholesterol content in proatherogenic LDL particles and decreased cholesterol levels in anti-atherogenic HDL particles (12). Studies investigating the genetic predisposition of “superagers” or “centenarians” with well-maintained health and cognitive performance revealed that polymorphisms that impair the activity of CETP are positively associated with longevity, cardiovascular health, and sustained cognitive performance (13–15). Based on these findings, several studies investigated whether *CETP* polymorphisms could decrease the risk for Alzheimer’s disease, an aging-associated neurodegenerative disease. Indeed, protective effects of *CETP* polymorphisms at early Alzheimer’s disease stages were reported, particularly in carriers of the strongest genetic risk factor, the $\epsilon 4$ allele of the *APOE4* (16–19). ApoE is the predominant lipoprotein of the brain, in contrast to the blood where there are several apolipoprotein-defined lipoprotein families (20). Those epidemiological findings indicate that CETP activity may impact on cognitive

*For correspondence: Lisa Marie Munter, lisa.munter@mcgill.ca.



performance and brain functions; however, the underlying mechanisms remain unclear.

While CETP is predominantly expressed in the liver and secreted to the blood, it is expressed in astrocytes as well (21). However, its function in the CNS remains elusive. Considering the important effect of CETP on systemic cholesterol levels, we hypothesized that CETP may also contribute to the alterations of the brain's cholesterol levels. It is important to note that mice naturally lack CETP, and therefore, they have considerably less LDL compared with humans (22). To gain insight on how CETP may impact on cognitive performance in humans, we used a well-established *CETP* transgenic (*CETP*^{tg}) mouse model expressing the human *CETP* gene under its natural promoter that is frequently used in the cardiovascular research field (23). The promoter contains a cholesterol-responsive element that induces *CETP* gene expression in response to dietary lipids. Therefore, *CETP* expression in *CETP*^{tg} mice leads to increased LDL levels and could thus be regarded as a mouse model with a humanized (normolipidemic) lipoprotein profile (24). We herein characterized the effects of *CETP* expression on molecular changes in the brain in *CETP*^{tg} mice. We observed higher cholesterol levels in the brains of *CETP*^{tg} as compared with wt mice. Transcriptome profiling of mostly astrocytes revealed no significant changes in cholesterol synthesis. However, we observed decreased cholesterol secretion and upregulation of the complement factor C1Q linked to neuronal cholesterol efflux (25).

MATERIALS AND METHODS

All experiments were conducted in accordance with McGill University environmental health and safety regulations as well as the Canadian biosafety standards and guidelines.

Western blot analysis of mouse tissue

Fresh-frozen liver or brain samples (approximately 100 mg) were lysed in 5× volume of lysis buffer (150 mM NaCl, 10% glycerol, 2 mM EDTA, 0.5% NP-40, 0.1% sodium deoxycholate, 20 mM Hepes, 1× cOmplete Protease Inhibitor Cocktail [Roche], pH 7.4) using lysing-matrix D at 6,000 rpm for 40 s. The lysates were diluted 1:5 in lysis buffer and prepared for SDS-PAGE (10% or 15%). Primary antibodies used were 22C11 (Millipore), anti-GAPDH (14C10; Cell Signaling), TP2 (kind gift of the Ottawa Heart Institute), anti-triggering receptor expressed in myeloid cells 2 (TREM2) (Mab1729; R&D Systems) and anti-ABCA7 (polyclonal; Thermo Fisher Scientific), and horseradish peroxidase-coupled secondary antibodies (Promega). Chemiluminescence images were acquired using the ImageQuant LAS 500 system (GE Healthcare).

RT-quantitative PCR

mRNA was isolated from mouse tissue (Macherey & Nagel). Briefly, 25–50 µg of fresh-frozen tissue were lysed in 450 µl RNA preparation buffer (with β-mercaptoethanol) in lysing-matrix D tubes using a MagNA Lyser (6,000 rpm 2× 30 s). RNA concentration was adjusted to 100 pg/ml, and 500 ng of

RNA were transcribed into complementary DNA (Applied Biosystems). RT-quantitative PCR (qPCR) was performed using the SsoAdvanced SYBR green supermix (Bio-Rad) on a Bio-Rad CFX384Touch cycler. All primers were obtained from integrated DNA technologies. *CETP* forward: CAGAT-CAGCCACTTGTCCAT, *CETP* reverse: CAGCTGTGTGTT-GATCTGGA; *Abca7* forward: TTCTCAGTCCCTCGTCA CCCAT, *Abca7* reverse: GCTCTTGTCTGAGGTTCCCTCGT; *Tnfa* forward: GGTGCCTATGTCTCAGCCTCTT, *Tnfa* reverse: GCCATAGAACTGATGAGAGGGAG; *Il1b* forward: TGGACCTTCCAGGATGAGGACA, *Il1b* reverse: GTTCAT CTCGGAGCTGTAGT; toll-like receptor 4 (*Tlr4*) forward: AGTTTCTCCAATTTTTCAGAAGCTTC, *Tlr4* reverse: TGA GAGGTGGTGTAAAGCCATGC; *Trem2* forward: ACAG-CACCTCCAGGAATCAAG, *Trem2* reverse: AACCTGCT-CAGGAGAACC GA; and *Il6* forward: CCTCTGGTCTTC TGGAGTACC, *Il6* reverse: ACTCCTTCTGTGACTCCAGC. Reference genes: *Hprt* forward: CCAGTTTCACTAATGACACAAACG, *Hprt* reverse: *Psmc4* forward: CCG CTTACACACTTCGAGCTGT, *Psmc4* reverse: GTGATG TGCCACAGCCTTTGCT; *Gapdh* forward: CATCACTGC-CACCCAGAAGACTG, *Gapdh* reverse: ATGCCAGT-GAGCTTCCCGTTCAG; and β-actin forward: CATTGCTG ACAGGATGCAGAAGG, β-actin reverse: TGCTGGAAGG TGGACAGTGAGG. Primer efficiency was determined to be between 90 and 110%.

Imaging mass spectrometry

Fresh-frozen brain samples were sectioned sagittally (Bregma; ~2.5) at 14 µm thickness and mounted on indium-tin-oxide-coated microscopy slides (Delta Technologies, Loveland, CO). Silver metal deposition was then performed on all slides using a Cressington 308R sputter coater (Ted Pella, Inc, Redding, CA) according to Dufresne *et al.* (26). A 20 nm silver layer thickness was determined to be optimal for maximum cholesterol signal intensity from brain tissue sections. Silver-assisted laser desorption ionization imaging mass spectrometry (IMS) data were acquired using a MALDI-TOF/TOF ultrafleXtreme mass spectrometer (Bruker Daltonics, Billerica, MA). Silver-assisted laser desorption ionization IMS data were visualized in flexImaging (4.1) without normalization (Bruker Daltonics, Billerica, MA). Relative intensities from the hippocampal region of each sample were calculated in R (version 3.4.4) with the Cardinal package (version 2.1) using the pipeline described by Yang *et al.* (27). Briefly, the raw data and manually selected regions of interest were exported from flexImaging as imzML or XML, respectively, and imported into R for preprocessing. The average intensities at *m/z* 493.2 (corresponding to the [M + Ag¹⁰⁷]⁺ silver adduct cholesterol ion) for each hippocampal region were then extracted based on the manually selected regions of interest and calculated. Significance was calculated with a Student's *t*-test.

Filipin staining and immunohistochemistry

Fresh-frozen brains were cut on the sagittal plane at 25 µm thickness using a cryostat (Leica, Germany). Sections were fixed in 4% paraformaldehyde at 4°C for 2 h. Filipin III was dissolved in dimethylformamide (10 mg/ml) and diluted 100-fold with 10 mM PBS. Sections were washed in PBS and incubated in 0.01 mg/ml Filipin complex solution (Sigma-Aldrich) at room temperature for 2 h. After washing with PBS, brain sections were mounted and imaged with Zeiss AxioImager M2 Imaging microscope with the Zeiss ZenPro

software, version 2.3 (Zeiss Canada). For immunohistochemistry, brain sections were permeabilized with 0.2% Triton-X in PBS and blocked for 1 h at room temperature in 10% normal donkey or goat serum. Sections were incubated in a cocktail of primary antibodies composed of mouse anti-gliofibrillary acidic protein (GFAP) (Cell signaling; catalog no.: 3670; 1:1,000 dilution), and rabbit anti-Clq (Abcam; catalog no.: ab182451; 1:400 dilution) prepared in 5% blocking solution for 12 h at 4°C. Primary antibody labeling was detected using species-specific secondary antibodies conjugated to Alexa 488 and Alexa 568 (Invitrogen; 1:800 dilution, incubated at room temperature for 2 h). Sections were mounted on gelatin subbed slides and coverslipped using Prolong Gold Antifade mounting medium (Invitrogen). Sections were imaged using Zeiss LSM 800 confocal microscope. Filipin and Clq fluorescence intensity levels were quantified by the average intensity of staining in ImageJ (National Institutes of Health) using images captured by 20× objective (Clq) and 40× objective (filipin). Specifically for filipin staining, all images were thresholded to an equal value that was determined empirically, and only fluorescent intensities corresponding to the cell membranes were quantified. All values were normalized to the background fluorescence of the corresponding image.

Mouse housing

The *CETP*^{tg} mouse strain B6.CBA-Tg(*CETP*)5203Tall/J (Jackson strain no.: 003904) (23) was housed according to the McGill University standard operating procedure mouse breeding colony management #608. All procedures were approved by McGill's Animal Care Committee and performed in accordance with the ARRIVE guidelines (Animal Research: Reporting in Vivo Experiments). The strain was maintained heterozygously, and nontransgenic littermates were served as controls. Genotyping was performed by Transnetyx. Diets: low fat control diet (TD.08485), low fat diet enriched with 1% cholesterol (TD.140215), and a diet containing 21% FAs and 1% cholesterol (TD.95286) (Envigo). The FA composition was 65% saturated FA, 31% MUFA, and 4% PUFA. Animals of both sexes were assigned randomly to treatment groups.

Plasma lipid analysis

The lipid analysis of mouse plasma samples was performed using the COBAS INTEGRA 400 Plus (Roche) and the following kits: COBAS INTEGRA CHOL 2, COBAS INTEGRA HDL-C gen3, and COBAS INTEGRA TRIG GPO 250, respectively. The levels of LDL-C were calculated using the Friedewald's formula: [total cholesterol] – [HDL-C] – [triglyceride/2.2].

CETP activity assay

CETP activity was measured using the Roar Biomedical, Inc fluorescent CETP activity assay. Here, 5 μ l of cell culture supernatant was incubated with 0.3 μ l donor and 0.3 μ l acceptor molecules in 30 μ l reaction volume. The reaction mix was incubated for 3 h at 37°C in a water bath, and the fluorescence (λ_{ex} 465/ λ_{em} 535) was measured.

Astrocyte enrichment

Astrocytes were enriched using the Anti-ACSA-2 MicroBead Kit (Miltenyi Biotec). Briefly, whole mouse brains

were dissociated using a miltenyi gentleMACS Octo dissociator with heaters, and ACSA-2-positive astrocytes were isolated using anti-ACSA-2 antibody magnetic beads according to the manufacturer's instructions. Enriched ACSA-2/GLAST-positive astrocytes were ethanol fixed, stained with a Cy3-labeled anti-GFAP antibody (1:1,000 dilution; Sigma), and analyzed on a BD LSRFortessa flow cytometer. BD FACSDIVA 8.0.1. was used for analysis.

Astrocyte microarray

RNA from enriched astrocytes was isolated using the Macherey & Nagel mRNA isolation kit. The Affymetrix clariom-S nano microarray was performed at the Genomecenter Quebec according to the manufacturer's instructions. The initial microarray dataset was analyzed using Transcriptome Analysis Software (Affymetrix).

Statistical analysis

Statistical analysis was performed using the GraphPad Prism 7 and 8 software (GraphPad Software, Inc). Analyses include only parametric tests: Student's *t*-test, two-way ANOVA followed by Bonferroni corrections, and Tukey's multiple comparison tests. All *P* values, statistical tests, *N* values, and the experimental units employed are indicated in figure legends.

RESULTS

Dietary cholesterol intake induces CETP expression

CETP^{tg} animals have been widely used in cardiovascular research (23). However, it remains unclear if FAs further induce CETP expression in addition to dietary cholesterol. To identify the ideal diet for inducing CETP expression in the *CETP*^{tg} model, we compared a diet enriched with 1% (w/w) cholesterol to a diet containing 1% cholesterol plus 21% (w/w) FAs (cholesterol/FA). Wt and *CETP*^{tg} mice received diets for 1 month starting at 2 months of age (Fig. 1A). As expected, *CETP*^{tg}, but not wt mice, showed CETP activity, confirming that there is no compensatory mechanism for the lack of CETP in wt mice. CETP activity was increased 2-fold in *CETP*^{tg} mice that were on a diet enriched in cholesterol or cholesterol/FA as compared with those on standard diet (Fig. 1B). Likewise, both high-fat diets induced a 2-fold increase of circulating CETP protein levels in mouse plasma, as determined by Western blot (Fig. 1D, E). Furthermore, we quantified *CETP* mRNA levels in liver by RT-qPCR and found that the diet supplemented only with cholesterol induced a bigger increase of *CETP* mRNA levels (8.8-fold) as compared with the high-cholesterol/FA diet (7-fold) (Fig. 1C). When assessing the lipid profile in plasma, we found that *CETP*^{tg} mice had lower HDL-C levels on standard and high-cholesterol diets, an effect that was missing in mice receiving the cholesterol/FA diet (Fig. 1F). LDL cholesterol levels were significantly elevated in *CETP*^{tg} animals fed with a cholesterol-enriched diet, which was not observed in animals fed with a cholesterol/FA diet, likely because of the

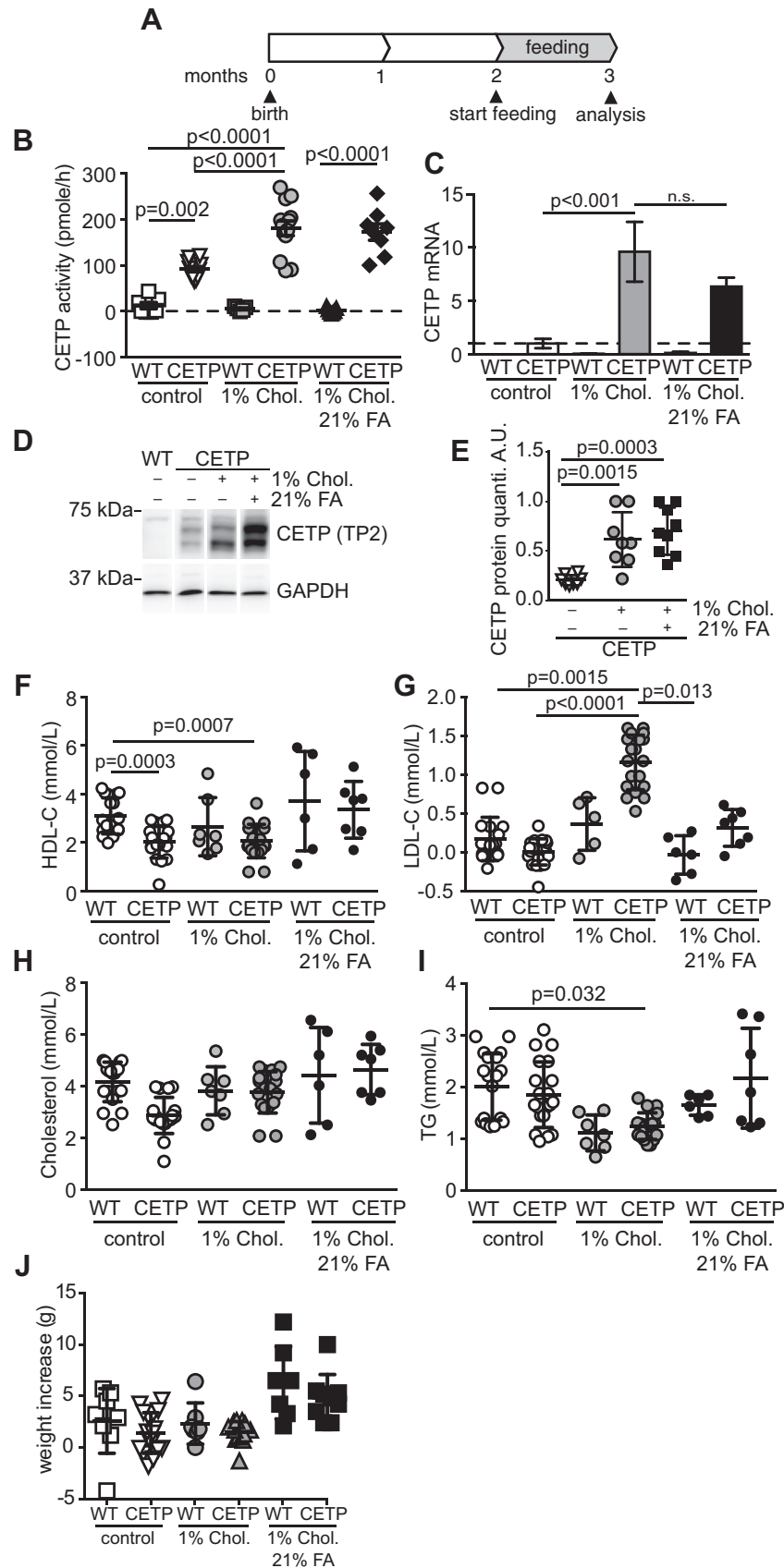


Fig. 1. Dietary cholesterol intake induces CETP expression. **A:** Feeding schedule and study design. Wt and *CETP*^g animals were fed for 1 month starting at the age of 2 months. Biochemical analyses were performed after 3 months of age. **B:** CETP activity of *CETP*^g or wt animals was measured from 1 μ l plasma using the fluorescence-based CETP activity assay (Roar Biomedical). $n = 6-14$, mean \pm SEM; 2-way ANOVA, Tukey's multiple comparison. **C:** Relative normalized *CETP* expression. RT-qPCR of liver samples at the age of

presence of monounsaturated and polyunsaturated FAs (28), although both diets led to a similar increase in CETP activity and protein levels (Fig. 1G). It is important to note that those LDL levels of approximately 1.2 mmol/l observed in *CETP*tg mice are still relatively low, given that human LDL levels <3 mmol/l are considered healthy. Total cholesterol was not significantly affected by the diets (Fig. 1H). However, we found a trend toward decreased levels of triglycerides in animals fed with the cholesterol diet independent of the genotype (Fig. 1I). Finally, we analyzed the net weight gain of mice during the 4-week diet period. In contrast to the cholesterol/FA diet, mice on the cholesterol diet did not show an additional weight gain as compared with standard diet (Fig. 1J). Together, high CETP expression and enhanced activity are achieved with both diets. However, the blood lipoprotein profile only changed toward a more human-like profile, that is, increased LDL levels, in mice receiving the cholesterol-only diet. In addition, since cholesterol-enriched food did not impact the weight of mice, this diet has the advantage that potentially confounding factors such as obesity can be excluded. Thus, we chose to use the 1% cholesterol diet for further experiments.

CETP promotes TREM2 expression in the liver

To ultimately study the chronic effect of CETP expression on the brain, we expanded the diet period to 3 months (Fig. 2A). First, we analyzed the effect of CETP on plasma LDL levels and transcriptional changes in the liver. Dietary cholesterol is known to decrease cholesterol synthesis and transcription of genes involved in cholesterol synthesis (the rate-limiting enzyme 3-hydroxy-3-methylglutaryl-coenzyme A reductase [*Hmgcr*]) and cholesterol uptake (*Ldlr* and the *Lrp1*) through regulation of SREBP-2 (29). Indeed, *Hmgcr*, *Ldlr*, and *Lrp1* mRNA levels were decreased on high-cholesterol diet in wt and *CETP*tg mice as compared with wt mice on a standard diet at the age of 5 months (Fig. 2B–D) (30). In addition, *CETP*tg mice on a standard diet showed lower *Hmgcr* and *Ldlr* gene expression levels as compared with wt as well, indicating that the little CETP expressed on a standard diet already redistributed cholesterol (Fig. 2B, C). In addition, we assessed two Alzheimer's risk genes, the *ABCA7*, a lipid transporter that is also regulated by SREBP-2, and *Trem2*, a lipoprotein receptor (31–34). *ABCA7* protein levels were double in *CETP*tg mice compared with wt mice in either diet and also doubled when either wt and *CETP*tg mice were put on a cholesterol diet. Thus, there was a 4-fold increased

difference in *ABCA7* protein levels between the extremes; that is, wt on standard diet compared with *CETP*tg on cholesterol diet (Fig. 2E–G). *Trem2* gene transcription was also increased by both the cholesterol diet and CETP expression leading to an 8-fold increase of transcript levels when comparing the two extremes (wt mice on standard diet with *CETP*tg mice on cholesterol diet) (Fig. 2H). However, this transcript increase could not be replicated at the protein level, which could be attributed to overall low signal intensities in the Western blot (Fig. 2E, I).

CETP activity promotes peripheral inflammation

It has been previously shown that cholesterol-enriched diets induce inflammation (35). Here, we assessed the effect of CETP as well as high-cholesterol diet on peripheral inflammation. Specifically, we quantified the inflammatory cytokines IL1 β and TNF α in mouse plasma samples using multiplex ELISA of 5-month-old mice after 3 months of a 1% cholesterol or control diet. TNF α levels were significantly increased in *CETP*tg mice as compared with wt mice on cholesterol diet; however, it should be noted that out of the 10 plasma samples analyzed, six samples had very low TNF α levels comparable to the control diets, and only four mice showed elevated TNF α levels (Fig. 3A). Levels of IL1 β were slightly increased in several *CETP*tg mice on the cholesterol diet, and one mouse had much higher levels (Fig. 3B). Since CETP is mainly secreted by the liver, we determined mRNA expression of such cytokines in the liver by qRT-PCR. As expected, the same mice with elevated plasma cytokine levels also had elevated *Tnfa* and *Il1b* mRNA levels in liver (Fig. 3C, D). Furthermore, mRNA expression of the *Tlr4* as upstream regulator of TNF α and IL1 β was also increased in mice with highest cytokine levels (Fig. 3E). Similarly, transcript levels of *Il6*, an interleukin that was reported to induce the expression of lipid-regulating proteins was high in 3 of 12 mice (Fig. 3F) (36). To analyze whether inflammatory cytokine production was extended to the CNS, transcript levels were determined from cortical samples. While we were able to demonstrate that CETP is expressed in the cortex of *CETP*tg mice, its expression levels were not affected by dietary cholesterol intake (Fig. 3G). Importantly, cytokine levels were not significantly increased in the brain at this age except for *Il1b* levels (Fig. 3H–J). In summary, CETP expression and a cholesterol diet induced inflammatory responses in the periphery, as expected, with attenuated effects in the brain.

5 months, n = 5–8, mean \pm SEM; 2-way ANOVA, Tukey's multiple comparison. D: CETP Western blot from liver lysates. Liver lysates were separated on 10% SDS-PAGE gels. CETP was detected using the TP2 monoclonal antibody. E: Quantification of CETP Western blots as shown in D: n = 8, mean \pm SEM; Student's *t*-test. F–I: Plasma lipoprotein analysis: F: HDL-C, G: LDL-C, H: total cholesterol, and I: triglycerides from mouse plasma samples. n = 6–14. Mean \pm SEM; 2-way ANOVA, Tukey's multiple comparison test. J: Mouse weight increase: Net weight increase of wt and *CETP*tg mice during the feeding period.

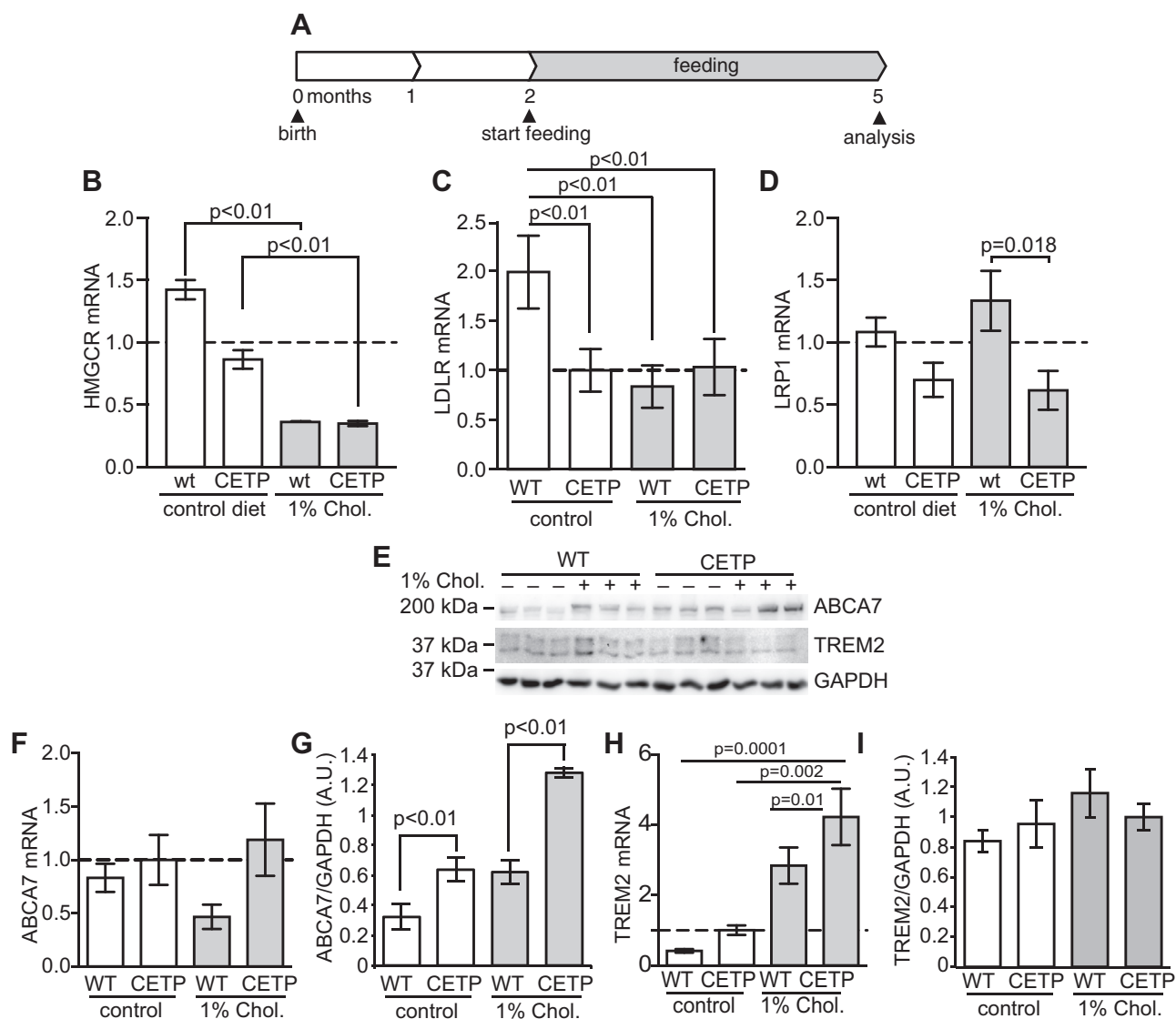


Fig. 2. CETP promotes ABCA7 and TREM2 expression in the liver. **A:** Feeding schedule and study design. Wt and *CETP*^{tg} mice were fed for 3 months starting at the age of 2 months. Biochemical analyses were performed at 5 months. **B–D:** Normalized RT-qPCR from mouse liver tissue. **B:** *Hmgcr*, **C:** *Ldlr*, and **D:** *Lrp1* expression, $n = 6–14$, mean \pm SEM; 2-way ANOVA, Tukey's multiple comparison test. **E:** Western blot analysis of ABCA7 and TREM2 from liver lysates. Antibodies used: rabbit-anti-GAPDH (14C10; Cell Signaling), anti-TREM2 (Mab1729; R&D Systems), and anti-ABCA7 (polyclonal; Thermo Fisher Scientific), $n = 6$; mean \pm SEM, Student's *t*-test. **F–I:** Expression analysis of ABCA7 and TREM2 from liver samples. Normalized RT-qPCR levels of liver **F:** *Abca7* and **H:** *Trem2*; $n = 6–14$, mean \pm SEM; 2-way ANOVA, Tukey's multiple comparison test. Western blot quantification of **G:** ABCA7 and **I:** TREM2; $n = 6$; mean \pm SEM, Student's *t*-test.

CETP changes the brain cholesterol composition

To determine the effect of CETP expression and high-cholesterol diet on the composition and distribution of lipids in the brain, we employed MALDI IMS. While several studies have looked at the distribution of lipids in the brain by IMS using 1,5-diaminonaphthalene or other organic matrices (37, 38), the visualization of cholesterol using IMS remained challenging. Here, we deposit a fine homogeneous silver layer over the tissue sections to promote the LDI and allow the imaging of cholesterol and olefin containing FAs with high specificity and sensitivity (26). The heatmap images depict the distribution of cholesterol in sagittal mouse brain sections detected at m/z 493 ($[M + Ag^{107}]^+$ silver adduct

molecular ion) (Fig. 4A). Cholesterol is found at the highest concentrations in the myelin-rich fiber tracts, whereas lower levels are observed in cortex, hippocampus, and cerebellum (Fig. 4A). Most interestingly, *CETP*^{tg} mice showed overall higher cholesterol levels in the brain than wt mice with a 22% increase in the hippocampal region (Fig. 4A–C). Cholesterol quantification from the whole brain section showed similar trends, albeit without statistical significance (Fig. 4D).

The hippocampus is a well-studied brain region responsible for critical brain functions such as memory consolidation, and its alterations are commonly associated with cognitive decline. To confirm the mass spectrometry results with a second independent approach

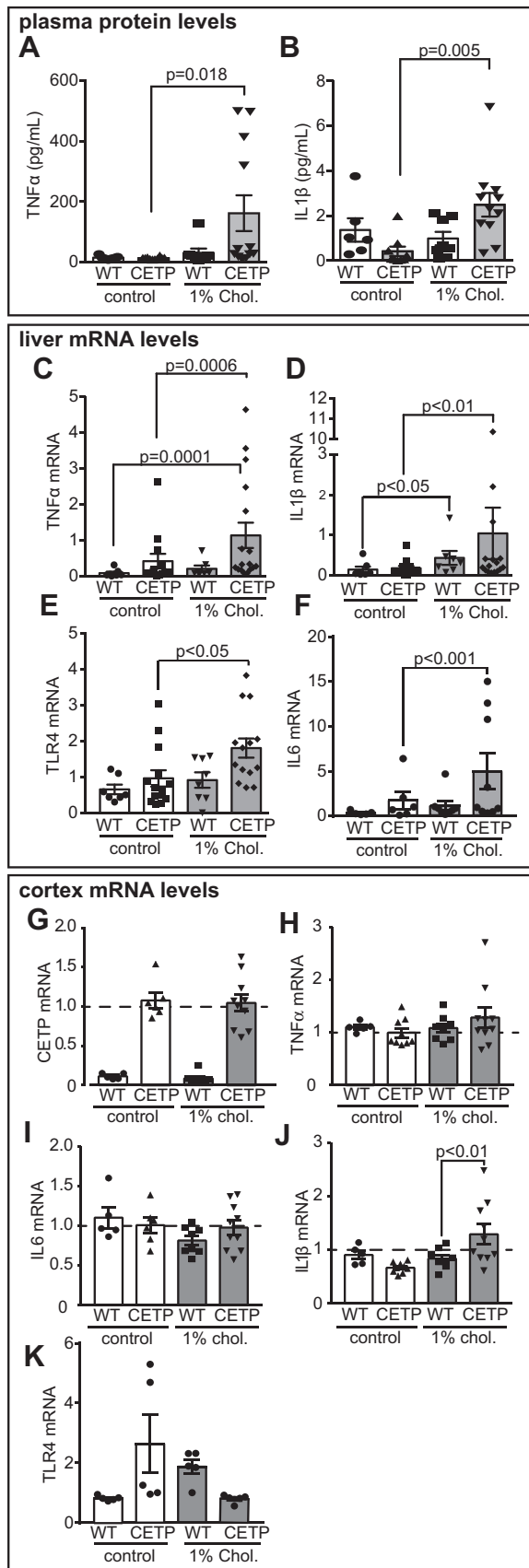


Fig. 3. CETP activity promotes peripheral inflammation. A and B: Plasma cytokine levels. A: TNF α and B: IL1 β measured in 25 μ l plasma using a multiplex ELISA (mesoscale discoveries); n = 6–11. Mean \pm SEM; 2-way ANOVA, Tukey’s multiple

and with higher resolution, we used filipin staining to assess cholesterol levels in the CA1, CA3, and dentate gyrus regions of hippocampus (Fig. 4E). Filipin staining in the hippocampus clearly labeled the plasma membranes in all conditions. The overall cholesterol levels assessed by intensity of filipin fluorescence was elevated by 15–25% in all hippocampal regions *CETP*tg mice as compared with wt mice on a high-cholesterol diet (Fig. 4G). Interestingly, the presence of CETP significantly increased cholesterol levels in the CA3 and dentate gyrus region of the cholesterol-diet group as compared with *CETP*tg on a standard chow, suggesting location-specific differences in cholesterol metabolism and/or transport (Fig. 4G). Furthermore, at a high magnification, we noticed accumulated cholesterol deposits in brain sections only of *CETP*tg mice on the cholesterol diet (Fig. 4F).

Transcriptomic profiling of enriched astrocytes by microarray

To investigate whether the increased brain cholesterol levels are a result of changes in the transcription of genes that induce cholesterol synthesis, we performed a microarray from enriched astrocyte mRNA (Fig. 5). The two extreme conditions of lowest and highest cholesterol content in the brain were chosen (i.e., wt mice on a control diet compared with *CETP*tg mice on cholesterol diet resulting in a ~22% cholesterol increase; Fig. 4C, G). Cells positive for the GLAST, a specific marker of astrocytes, were enriched from freshly dissected and dissociated whole brains using the ACSA-2 MicroBead Kit. To verify the enrichment of astrocytes, approximately 8×10^5 cells were stained for the astrocyte marker, GFAP, and analyzed by flow cytometry revealing an enrichment of more than 70% across all samples (Fig. 5A). Using total purified mRNA from such enriched cells, *CETP* expression was validated in the mRNA by qPCR (Fig. 5B). Transcripts were analyzed on a Clariom S microarray. About 410 genes were significantly upregulated and 814 genes significantly downregulated at a log₂ fold change threshold level of 0.5 (Fig. 5C, D). Genes involved in cholesterol synthesis were not regulated except for mevalonate kinase (*Mvk*) and lanosterol synthase (*Lss*), which were upregulated, and hydroxysteroid (17- β) dehydrogenase 7 (*Hsd17b7*), which was downregulated (Fig. 5E). Overall, these data imply that it is unlikely that increased de novo cholesterol synthesis is responsible for the elevated cholesterol levels in *CETP*tg mice.

comparison test. C–F: RT-qPCR of liver samples from 5-month-old mice. Normalized expression of: C: TNF α , D: IL1 β , E: TLR4, and F: IL6 expression; n = 6–14, mean \pm SEM; 2-way ANOVA, Tukey’s multiple comparison test. G–K: Cytokine mRNA expression in brain samples by normalized RT-qPCR: G: CETP, H: TNF α , I: IL6, J: IL1 β , and K: TLR4 expression; n = 6–10. Mean \pm SEM; 2-way ANOVA, Tukey’s multiple comparison test.

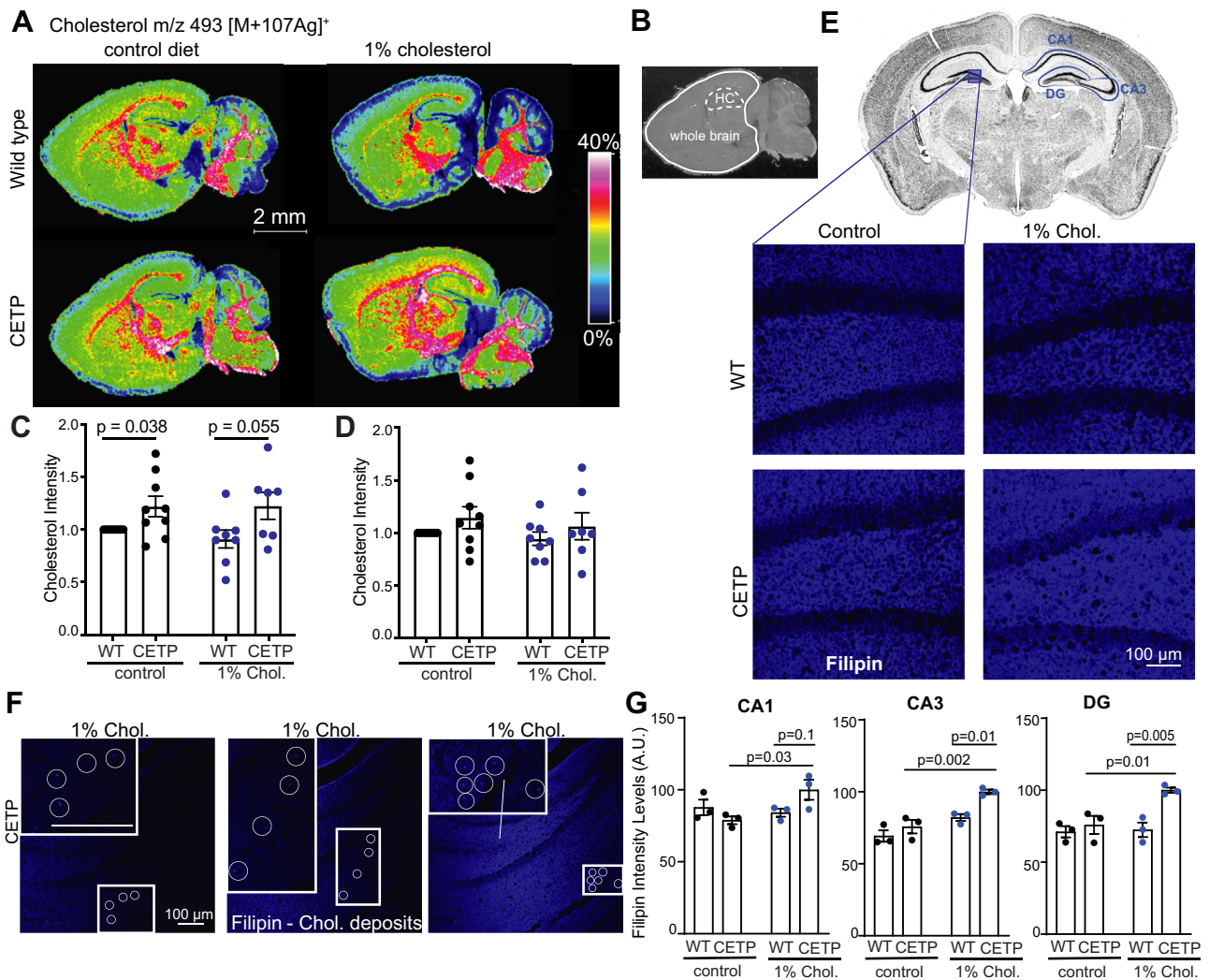


Fig. 4. CETP changes the brain cholesterol composition. **A:** MALDI IMS on sagittal brain sections of 5-month-old wt and *CETP*g brains. Heatmap representation of peak intensities corresponding to cholesterol (m/z 493 $[M + Ag^{107}]^+$). **B:** Whole brain sagittal section representing regions of interest selected for “whole brain” or hippocampal (HC) quantification. **C, D:** Quantification of peak intensities corresponding to cholesterol from hippocampus (**C**) or whole brain (**D**); $n = 7-9$, mean \pm SEM, 1-way ANOVA following Bonferroni’s multiple comparison *t*-test. **E:** Coronal view of mouse brain section showing hippocampal regions of CA1, CA3, and DG. The blue inset shows the portion of DG that was selected for demonstrating representative images. Representative images of filipin staining in brain sections of wt and *CETP*g mice on standard and high-cholesterol diet. **F:** Consecutive confocal stacks from the hippocampus of 1% cholesterol-fed *CETP*g mice showing multiple filipin-bound cholesterol deposits. Insets show enlarged views of areas with cholesterol deposits. **G:** Quantifications of filipin fluorescent intensities in different hippocampal regions shown in **E**; $n = 3$, mean \pm SEM, two-way ANOVA followed by Bonferroni’s multiple comparisons test. Scale bars represent 100 μ m.

Amongst the genes with high upregulation were the three encoding for the Clq complex, the initiating factor of the classic complement cascade (Fig. 5C). Clq is an important marker of neurodegeneration and may contribute to synapse loss in Alzheimer’s disease (39, 40). Diverse functions are attributed to Clq and interestingly also one relating to cholesterol extraction from neurons (25, 41). To reveal if the potential expression changes in Clq subunit genes are relevant at the protein level, we performed immunohistochemistry on hippocampal sections for Clq revealing a significant increase in Clq protein expression throughout the hippocampus of high-cholesterol-fed *CETP*g mice compared with wt and *CETP*g mice on a normal diet (Fig. 5F,G). Given that Clq

promotes neuronal cholesterol clearance, increased Clq levels in *CETP*g mice on high cholesterol may be a compensatory reaction to promote excess cholesterol clearance in the brains of these mice.

To investigate the cause of increased brain cholesterol levels, we considered decreased cholesterol excretion through the blood-brain barrier. Therefore, we quantified 24S-hydroxycholesterol in the brain, a cholesterol metabolite generated by the neuronally expressed enzyme CYP46A1, and which can freely diffuse over the blood-brain barrier and excrete cholesterol from the brain at a rate of about 6 mg per day (42, 43). We indeed observed a significant 14% reduction of 24S-hydroxycholesterol in *CETP*g mice

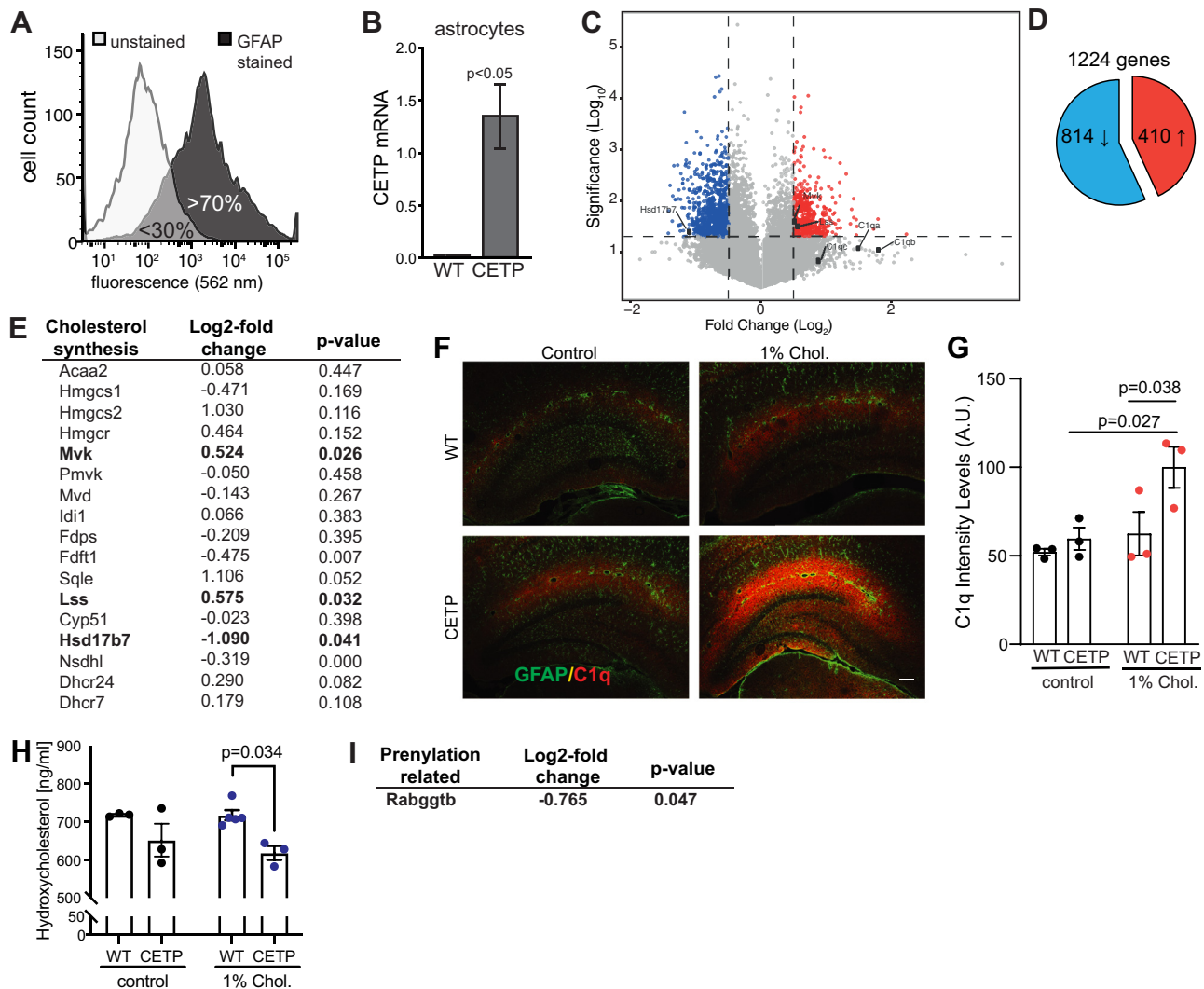


Fig. 5. Transcriptional changes in *CETP*g brain. **A:** Flow cytometry analysis of astrocyte enrichment from 5-month-old mouse brains. Astrocytes were stained with GFAP. More than 70% of purified cells were GFAP positive. **B:** *CETP* RT-qPCR of astrocyte-enriched mRNA, $n = 2-3$. Mean \pm SEM; 2-way ANOVA. **C:** Volcano plot of the mouse microarray results. Each dot represents an individual gene. The P value was plotted against the fold change of the corresponding gene. P values cutoff for significance was set to <0.05 . **D:** Overall, 410 genes were found to be significantly upregulated and 814 genes were found to be significantly downregulated in our dataset. **E:** Genes involved in the de novo synthesis of cholesterol. **F:** Representative images of astrocytes (green) and Clq (red) immunostaining in brain sections of wt and *CETP*g mice on normal and high-cholesterol diet. **G:** Quantifications of Clq fluorescent intensities in hippocampus $n = 3$, mean \pm SEM, two-way ANOVA followed by Bonferroni's multiple comparisons test. Scale bar represents 100 μ m. **H:** ELISA quantification of 24S-hydroxycholesterol from brain extracts; $n = 3$, mean \pm SEM, one-way ANOVA followed by Bonferroni's multiple comparisons test. **I:** Gene involved in geranylation; *Rabggtb*, Rab geranylgeranyl transferase β .

versus wt on a high-cholesterol diet (Fig. 5H). Thus, we conclude that the elevated cholesterol levels in *CETP*g brain are likely caused by cholesterol accumulation over weeks because of defective efflux. Together, increased Clq expression may indicate cholesterol accumulation in neurons, and decreased 24S-hydroxycholesterol formation may indicate defective clearance from the brain explaining the overall high cholesterol levels in the brains of *CETP*g mice.

Furthermore, findings by the laboratory of David Russel suggested that a consequence of cholesterol accumulation could be the downregulation of de novo cholesterol synthesis and with it the downregulation of

farnesyl and geranyl precursors, which are required for post-translational modifications contributing to long-term potentiation and cognitive performance (44). In agreement with this idea, we found *Rabggtb* expression significantly downregulated, suggesting that geranylation may indeed be defective in *CETP*g mice on a cholesterol diet (Fig. 5I).

DISCUSSION

CETP-mediated increase in brain cholesterol

In this study, we aimed to understand effects of CETP on brain lipid composition and gene regulation

(Fig. 6). *CETP*g mice on a 1% cholesterol diet show a lipoprotein profile in the blood that better recapitulates the human lipoprotein profile and importantly shows a ~22% increase in brain cholesterol levels as compared with wt. Some *CETP*g mice on the cholesterol diet showed peripheral inflammation but no elevated cytokine levels in total cortical mRNA, except for *Iilb* at 5 months of age and after a 3-month long 1% cholesterol diet. The enhanced inflammatory response in liver and plasma could be attributed to higher cholesterol levels in immune cells, where it was already demonstrated that cholesterol augments, for instance, TLR receptor signaling, and modulates immune cells surrounding tumors (45, 46). To uncover the effect of CETP on gene regulation in the brain, we profiled transcriptomic changes in mostly astrocytes of the brains of *CETP*g mice on high cholesterol compared with wt mice on a normal diet. Here, it is important to note that our astrocyte-enrichment strategy led to a cell population of 70% astrocytes only, so that some of the regulated genes may result from copurified other cells. We then further focused on the complement factor Clq given its role in Alzheimer's disease, inflammation, and cholesterol clearance (25, 39, 40). Clq is elevated in *CETP*g mice on the cholesterol diet as compared with wt (Fig. 5C). Clq was originally viewed as the initiating component of the classical complement pathway. However, there is increasing evidence suggesting various complement-independent roles for Clq in innate and acquired immunity as well as neuronal plasticity (41). As such, Clq mediates synapse pruning, and it is also associated with neuroprotective effects such as the upregulation of cholesterol metabolism genes and decreasing cellular cholesterol content (25, 39). Thus, the elevated Clq levels in *CETP*g mice could be a reaction to the elevated cholesterol levels aiming to eliminate excess cholesterol from the brain.

We investigated if the increase of brain cholesterol arises from de novo synthesis in the brain, which we could not confirm by transcriptome analysis. The elevated cholesterol levels may be explained by one of the following alternative pathways. Some lipid exchange between the brain and the blood can occur (2, 47, 48). It is well established that beneficial dietary w3-FAs enter the brain (49, 50). APOAI and HDL

particles in in vitro assays were described to be capable of transporting cholesterol into the brain via scavenger receptor-mediated transport or transcytosis (51, 52). In addition, 24S- and 27-hydroxysterols efficiently cross the blood-brain barrier, and polymorphisms in 24S-hydroxylase CYP46A1 are associated with Alzheimer's disease (2, 42). Importantly, about 80% of 24S-hydroxycholesterol stems from neurons, and its efflux from the brain equals about 6 mg of cholesterol in an adult brain (42, 43). Since we determined lower 24S-hydroxycholesterol in *CETP*g mice, decreased cholesterol efflux from the brain likely explains the high cholesterol levels in the brains of *CETP*g mice.

While CETP shuttles cholesterol between HDL and VLDL in the blood, those lipoprotein particles do not exist in the brain (7). In the brain, APOE is the predominant lipoprotein, and most lipoprotein particles are HDL like in size and decorated with APOE or APOJ (8, 53). While a role for CETP in the brain is not clear, it is likely that it is active as a lipid transporter. However, the interaction partners may differ, and it is a possibility that CETP is involved in cholesterol redistribution between cells or acts as intracellular shuttle between organelles. Furthermore, CETP may be involved in the storage of lipids in microglia and astrocytes. In this line, the Morton laboratory reported a role of CETP in lipid droplet formation (54, 55). We observed cholesterol accumulations in brain sections of *CETP*g mice on cholesterol diet (Fig. 4F); however, further analysis is required to determine the exact nature of such accumulations. Consequently, it is possible that lifetime exposure to CETP activity in the brain may cause an overall retention of cholesterol in the brain through downregulation of 24S-hydroxycholesterol formation, leading to increased Clq expression as a compensatory mechanism (Fig. 6). It will be most interesting to reveal if blood-derived CETP, centrally expressed CETP, or both are responsible for the molecular changes of the brain described herein.

In the liver of *CETP*g mice, we observed an upregulation of ABCA7 and TREM2 as compared with wt mice. Mutations in both ABCA7 and TREM2 are known to be risk factors for Alzheimer's disease (32, 33). Two recent publications linked ABCA7 and TREM2 to bile

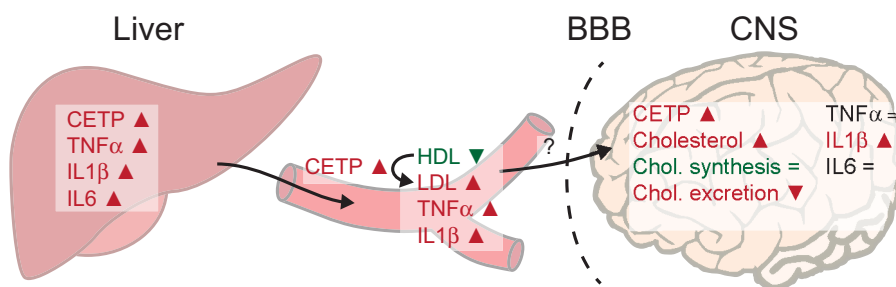



Fig. 6. CETP-mediated changes. Schematic representation of changes observed in liver, plasma, and brain in *CETP*g animals as compared with wt.

acid formation in the liver (56, 57). Thus, the elevated ABCA7 and TREM2 levels in *CETP*^{tg} mice in the liver may reflect an increase in bile acid formation. TREM2 is primarily regarded as not only an immune receptor in the brain but also acts as a lipoprotein receptor, particularly for APOE-containing particles (58–60). It is therefore tempting to speculate that ABCA7 and TREM2 may also be involved in cholesterol transport or redistribution in the brain.

To investigate neurodegenerative diseases linked to abnormal cholesterol content in the brain such as Alzheimer's, Parkinson's, and Huntington's disease as well as amyotrophic lateral sclerosis (61), it will be important to consider that all current respective mouse models lack CETP and may thus not fully represent cholesterol metabolic changes in the brain, which may be consequently underestimated. We suggest that mouse models expressing CETP will be a valuable tool to unravel the molecular mechanisms between peripheral and central cholesterol metabolism and neurodegeneration (61).

Data availability

The microarray data have been deposited at Gene Expression Omnibus datasets, accession number GSE111242. All other data are provided in the article. 




Acknowledgments

The authors thank Elizabeth-Ann Kranjec for initial MALDI IMS measures and Dr Scott Kiss, Dr Sandra Paschowsky, and Sassen Efrem for valuable feedback on the article. Image acquisition and processing for this manuscript was performed in the McGill University Advanced Bio-Imaging Facility (ABIF), RRID:SCR_017697.

Author contributions

F. O. conceptualization; F. O. methodology; Z. S. N. and A. N. validation; F. O., J. P., A. N., and A. V. C. formal analysis; F. O., N. Y., E. Y., J. P., and Z. S. N. investigation; F. O. resources; F. O. writing—original draft; N. Y., E. Y., J. P., A. N., P. C., and L. M. M. writing—review & editing; F. O. visualization; A. R.-d.-S., P. C., and L. M. M. supervision; L. M. M. funding acquisition.

Author ORCIDs

Jasmine Phénix  <https://orcid.org/0000-0002-5762-6376>
Albert Nitu  <https://orcid.org/0000-0001-9805-9622>
Lisa Marie Munter  <https://orcid.org/0000-0001-5736-1462>

Funding and additional information

This work was funded by the Alzheimer Society of Canada Young Investigator grant (grant no.: PT-58872) and regular research grant (grant no.: 17-02), the Weston Brain Institute award (grant no.: RR172187), and the Canadian Institute of Health Research (grant no.: CIHR-PJT-162302), and was supported by the Fonds de recherche du Québec - santé FRQS research allocation (grant no.: FRQ-S 36571), the Canada Foundation of Innovation Leaders Opportunity Fund grant (grant no.: 32565), and Natural Sciences and Engineering Research Council of Canada Discovery grants (grant nos.: RGPIN-2015-04645; to L. M. M. and RGPIN-2015-06802; to

P. C.). A. R.-d.-S. acknowledges support from the Canadian Institute of Health Research project grant (grant no.: PJT-166195). F. O. received studentships through the Integrated Program in Neuroscience and from the Canada First Research Excellence Fund, awarded to McGill University for the Healthy Brains for Healthy Lives initiative. N. Y. was the recipient of a doctoral studentship from the Louise and Alan Edwards Foundation. E. Y. received a doctoral studentship from Natural Sciences and Engineering Research Council of Canada. J. P. received a Healthy Brains, Healthy Lives Master's Fellowship award. A. V. C. received an Integrated Program in Neuroscience studentship award.

Conflict of interest

The authors declare that they have no conflicts of interest with the contents of this article.

Abbreviations

APOE, apolipoprotein E; CETP, cholesteryl ester transfer protein; CETP^{tg}, CETP transgenic; GFAP, glial fibrillary acidic protein; GLAST, glutamate aspartate transporter; HMGCR, 3-hydroxy-3-methylglutaryl-coenzyme A reductase; IMS, imaging mass spectrometry; LDLR, LDL receptor; LRP1, LDLR-related protein 1; qPCR, quantitative PCR; TLR4, toll-like receptor 4; TREM2, triggering receptor expressed in myeloid cells 2.

Manuscript received April 6, 2021, and in revised from June 28, 2022. Published, JLR Papers in Press, July 31, 2022, <https://doi.org/10.1016/j.jlr.2022.100260>

REFERENCES

1. Dietschy, J. (2009) Central nervous system: cholesterol turnover, brain development and neurodegeneration. *Biol. Chem.* **390**, 287–293
2. Bjorkhem, I., and Meaney, S. (2004) Brain cholesterol: long secret life behind a barrier. *Arterioscler. Thromb. Vasc. Biol.* **24**, 806–815
3. Yao, Z., and McLeod, R. S. (1994) Synthesis and secretion of hepatic apolipoprotein B-containing lipoproteins. *Biochim. Biophys. Acta.* **1212**, 152–166
4. Glomset, J. A. (1980) High-density lipoproteins in human health and disease. *Adv. Intern. Med.* **25**, 91–116
5. Liu, M., Kuhel, D. G., Shen, L., Hui, D. Y., and Woods, S. C. (2012) Apolipoprotein E does not cross the blood-cerebrospinal fluid barrier, as revealed by an improved technique for sampling CSF from mice. *Am. J. Physiol. Regul. Integr. Comp. Physiol.* **303**, R903–908
6. Vance, J. (2012) Dysregulation of cholesterol balance in the brain: contribution to neurodegenerative diseases. *Dis. Model. Mech.* **5**, 746–755
7. Vance, J., Hayashi, H., and Karten, B. (2005) Cholesterol homeostasis in neurons and glial cells. *Semin. Cell Dev. Biol.* **16**, 193–212
8. Vance, J. E., and Hayashi, H. (2010) Formation and function of apolipoprotein E-containing lipoproteins in the nervous system. *Biochim. Biophys. Acta.* **1801**, 806–818
9. Holtzman, D., Herz, J., and Bu, G. (2012) Apolipoprotein e and apolipoprotein e receptors: normal biology and roles in Alzheimer disease. *Cold Spring Harb. Perspect. Med.* **2**, a006312
10. Zilversmit, D. B., Hughes, L. B., and Balmer, J. (1975) Stimulation of cholesterol ester exchange by lipoprotein-free rabbit plasma. *Biochim. Biophys. Acta.* **409**, 393–398
11. Chajek, T., and Fielding, C. J. (1978) Isolation and characterization of a human serum cholesteryl ester transfer protein. *Proc. Natl. Acad. Sci. U. S. A.* **75**, 3445–3449
12. Lagrost, L. (1994) Regulation of cholesteryl ester transfer protein (CETP) activity: review of in vitro and in vivo studies. *Biochim. Biophys. Acta.* **1215**, 209–236

13. Zhong, S., Sharp, D. S., Grove, J. S., Bruce, C., Yano, K., Curb, J. D., *et al.* (1996) Increased coronary heart disease in Japanese-American men with mutation in the cholesteryl ester transfer protein gene despite increased HDL levels. *J. Clin. Invest.* **97**, 2917–2923
14. Barzilai, N., Atzmon, G., Derby, C., Bauman, J., and Lipton, R. (2006) A genotype of exceptional longevity is associated with preservation of cognitive function. *Neurology*. **67**, 2170–2175
15. Barzilai, N., Atzmon, G., Schechter, C., Schaefer, E., Cupples, A., Lipton, R., *et al.* (2003) Unique lipoprotein phenotype and genotype associated with exceptional longevity. *JAMA*. **290**, 2030–2040
16. Rodriguez, E., Mateo, I., Infante, J., Llorca, J., Berciano, J., and Combarros, O. (2006) Cholesteryl ester transfer protein (CETP) polymorphism modifies the Alzheimer's disease risk associated with APOE epsilon4 allele. *J. Neurol.* **253**, 181–185
17. Sanders, A., Wang, C., Katz, M., Derby, C., Barzilai, N., Ozelius, L., *et al.* (2010) Association of a functional polymorphism in the cholesteryl ester transfer protein (CETP) gene with memory decline and incidence of dementia. *JAMA*. **303**, 150–158
18. Sundermann, E. E., Wang, C., Katz, M., Zimmerman, M. E., Derby, C. A., Hall, C. B., *et al.* (2016) Cholesteryl ester transfer protein genotype modifies the effect of apolipoprotein epsilon4 on memory decline in older adults. *Neurobiol. Aging*. **41**, 200.e7–200.e12
19. Murphy, E. A., Roddey, J. C., McEvoy, L. K., Holland, D., Hagler, D. J., Jr., Dale, A. M., *et al.* (2012) CETP polymorphisms associate with brain structure, atrophy rate, and Alzheimer's disease risk in an APOE-dependent manner. *Brain Imaging Behav.* **6**, 16–26
20. Wang, H., and Eckel, R. H. (2014) What are lipoproteins doing in the brain? *Trends Endocrinol. Metab.* **25**, 8–14
21. Yamada, T., Kawata, M., Arai, H., Fukasawa, M., Inoue, K., and Sato, T. (1995) Astroglial localization of cholesteryl ester transfer protein in normal and Alzheimer's disease brain tissues. *Acta Neuropathol.* **90**, 633–636
22. Steenbergen, R. H., Joyce, M. A., Lund, G., Lewis, J., Chen, R., Barsby, N., *et al.* (2010) Lipoprotein profiles in SCID/uPA mice transplanted with human hepatocytes become human-like and correlate with HCV infection success. *Am. J. Physiol. Gastrointest. Liver Physiol.* **299**, G844–G854
23. Jiang, X., Agellon, L., Walsh, A., Breslow, J., and Tall, A. (1992) Dietary cholesterol increases transcription of the human cholesteryl ester transfer protein gene in transgenic mice. Dependence on natural flanking sequences. *J. Clin. Invest.* **90**, 1290–1295
24. Gauthier, B., Robb, M., Gaudet, F., Ginsburg, G. S., and McPherson, R. (1999) Characterization of a cholesterol response element (CRE) in the promoter of the cholesteryl ester transfer protein gene: functional role of the transcription factors SREBP-1a, -2, and YY1. *J. Lipid Res.* **40**, 1284–1293
25. Benoit, M. E., and Tenner, A. J. (2011) Complement protein C1q-mediated neuroprotection is correlated with regulation of neuronal gene and microRNA expression. *J. Neurosci.* **31**, 3459–3469
26. Dufresne, M., Thomas, A., Breault-Turcot, J., Masson, J. F., and Chaurand, P. (2013) Silver-assisted laser desorption/ionization for high spatial resolution imaging mass spectrometry of olefins from thin tissue sections. *Anal. Chem.* **85**, 3318–3324
27. Yang, E., Fournelle, F., and Chaurand, P. (2020) Silver spray deposition for AgLDI imaging MS of cholesterol and other olefins on thin tissue sections. *J. Mass Spectrom.* **55**, e4428
28. Fernandez, M. L., and West, K. L. (2005) Mechanisms by which dietary fatty acids modulate plasma lipids. *J. Nutr.* **135**, 2075–2078
29. Brown, M. S., Ye, J., Rawson, R. B., and Goldstein, J. L. (2000) Regulated intramembrane proteolysis: a control mechanism conserved from bacteria to humans. *Cell*. **100**, 391–398
30. Llorente-Cortes, V., Costales, P., Bernues, J., Camino-Lopez, S., and Badimon, L. (2006) Sterol regulatory element-binding protein-2 negatively regulates low density lipoprotein receptor-related protein transcription. *J. Mol. Biol.* **359**, 950–960
31. Wang, Y., Cella, M., Mallinson, K., Ulrich, J. D., Young, K. L., Robinette, M. L., *et al.* (2015) TREM2 lipid sensing sustains the microglial response in an Alzheimer's disease model. *Cell*. **160**, 1061–1071
32. Hollingworth, P., Harold, D., Sims, R., Gerrish, A., Lambert, J. C., Carrasquillo, M. M., *et al.* (2011) Common variants at ABCA7, MS4A6A/MS4A4E, EPHA1, CD33 and CD2AP are associated with Alzheimer's disease. *Nat. Genet.* **43**, 429–435
33. Guerreiro, R., Wojtas, A., Bras, J., Carrasquillo, M., Rogaeva, E., Majounie, E., *et al.* (2013) TREM2 variants in Alzheimer's disease. *N. Engl. J. Med.* **368**, 117–127
34. Iwamoto, N., Abe-Dohmae, S., Sato, R., and Yokoyama, S. (2006) ABCA7 expression is regulated by cellular cholesterol through the SREBP2 pathway and associated with phagocytosis. *J. Lipid Res.* **47**, 1915–1927
35. Wouters, K., van Gorp, P. J., Bieghs, V., Gijbels, M. J., Duimel, H., Lutjohann, D., *et al.* (2008) Dietary cholesterol, rather than liver steatosis, leads to hepatic inflammation in hyperlipidemic mouse models of nonalcoholic steatohepatitis. *Hepatology*. **48**, 474–486
36. Muller, N., Schulte, D. M., Turk, K., Freitag-Wolf, S., Hampe, J., Zeuner, R., *et al.* (2015) IL-6 blockade by monoclonal antibodies inhibits apolipoprotein (a) expression and lipoprotein (a) synthesis in humans. *J. Lipid Res.* **56**, 1034–1042
37. Thomas, A., Charbonneau, J. L., Fournaise, E., and Chaurand, P. (2012) Sublimation of new matrix candidates for high spatial resolution imaging mass spectrometry of lipids: enhanced information in both positive and negative polarities after 1,5-diaminonaphthalene deposition. *Anal. Chem.* **84**, 2048–2054
38. Caughlin, S., Park, D. H., Yeung, K. K., Cechetto, D. F., and Whitehead, S. N. (2017) Sublimation of DAN matrix for the detection and visualization of gangliosides in rat brain tissue for MALDI imaging mass spectrometry. *J. Vis. Exp.* <https://doi.org/10.3791/55254>
39. Hong, S., Beja-Glasser, V. F., Nfonoyim, B. M., Frouin, A., Li, S., Ramakrishnan, S., *et al.* (2016) Complement and microglia mediate early synapse loss in Alzheimer mouse models. *Science*. **352**, 712–716
40. Afagh, A., Cummings, B. J., Cribbs, D. H., Cotman, C. W., and Tenner, A. J. (1996) Localization and cell association of C1q in Alzheimer's disease brain. *Exp. Neurol.* **138**, 22–32
41. Thielsens, N. M., Tedesco, F., Bohlson, S. S., Gaboriau, C., and Tenner, A. J. (2017) C1q: a fresh look upon an old molecule. *Mol. Immunol.* **89**, 73–83
42. Bjorkhem, I. (2006) Crossing the barrier: oxysterols as cholesterol transporters and metabolic modulators in the brain. *J. Intern. Med.* **260**, 493–508
43. Sodero, A. O. (2021) 24S-hydroxycholesterol: cellular effects and variations in brain diseases. *J. Neurochem.* **157**, 899–918
44. Kotti, T., Head, D. D., McKenna, C. E., and Russell, D. W. (2008) Biphasic requirement for geranylgeraniol in hippocampal long-term potentiation. *Proc. Natl. Acad. Sci. U. S. A.* **105**, 11394–11399
45. Yang, W., Bai, Y., Xiong, Y., Zhang, J., Chen, S., Zheng, X., *et al.* (2016) Potentiating the antitumor response of CD8(+) T cells by modulating cholesterol metabolism. *Nature*. **531**, 651–655
46. Tall, A. R., and Yvan-Charvet, L. (2015) Cholesterol, inflammation and innate immunity. *Nat. Rev. Immunol.* **15**, 104–116
47. Bjorkhem, I., Lutjohann, D., Diczfalussy, U., Stahl, L., Ahlborg, G., and Wahren, J. (1998) Cholesterol homeostasis in human brain: turnover of 24S-hydroxycholesterol and evidence for a cerebral origin of most of this oxysterol in the circulation. *J. Lipid Res.* **39**, 1594–1600
48. Zlokovic, B. V. (2008) The blood-brain barrier in health and chronic neurodegenerative disorders. *Neuron*. **57**, 178–201
49. Nguyen, L. N., Ma, D., Shui, G., Wong, P., Cazenave-Gassiot, A., Zhang, X., *et al.* (2014) Mfsd2a is a transporter for the essential omega-3 fatty acid docosahexaenoic acid. *Nature*. **509**, 503–506
50. Ouellet, M., Emond, V., Chen, C. T., Julien, C., Bourasset, F., Oddo, S., *et al.* (2009) Diffusion of docosahexaenoic and eicosapentaenoic acids through the blood-brain barrier: an in situ cerebral perfusion study. *Neurochem. Int.* **55**, 476–482
51. Balazs, Z., Panzenboeck, U., Hammer, A., Sovic, A., Quehenberger, O., Malle, E., *et al.* (2004) Uptake and transport of high-density lipoprotein (HDL) and HDL-associated alpha-tocopherol by an in vitro blood-brain barrier model. *J. Neurochem.* **89**, 939–950
52. Stukas, S., Robert, J., Lee, M., Kulic, I., Carr, M., Tourigny, K., *et al.* (2014) Intravenously injected human apolipoprotein A-I rapidly enters the central nervous system via the choroid plexus. *J. Am. Heart Assoc.* **3**, e001156
53. Fagan, A. M., Holtzman, D. M., Munson, G., Mathur, T., Schneider, D., Chang, L. K., *et al.* (1999) Unique lipoproteins secreted by primary astrocytes from wild type, apoE (-/-), and human apoE transgenic mice. *J. Biol. Chem.* **274**, 30001–30007

54. Izem, L., and Morton, R. (2001) Cholesteryl ester transfer protein biosynthesis and cellular cholesterol homeostasis are tightly interconnected. *J. Biol. Chem.* **276**, 26534–26541
55. Izem, L., and Morton, R. (2007) Possible role for intracellular cholesteryl ester transfer protein in adipocyte lipid metabolism and storage. *J. Biol. Chem.* **282**, 21856–21865
56. MahmoudianDehkordi, S., Arnold, M., Nho, K., Ahmad, S., Jia, W., Xie, G., *et al* (2019) Altered bile acid profile associates with cognitive impairment in Alzheimer's disease-an emerging role for gut microbiome. *Alzheimers Dement.* **15**, 76–92
57. Nho, K., Kueider-Paisley, A., MahmoudianDehkordi, S., Arnold, M., Risacher, S. L., Louie, G., *et al* (2019) Altered bile acid profile in mild cognitive impairment and Alzheimer's disease: relationship to neuroimaging and CSF biomarkers. *Alzheimers Dement.* **15**, 232–244
58. Kober, D. L., Stuchell-Brereton, M. D., Kluender, C. E., Dean, H. B., Strickland, M. R., Steinberg, D. F., *et al* (2020) Functional insights from biophysical study of TREM2 interactions with apoE and Abeta1-42. *Alzheimers Dement.* <https://doi.org/10.1002/alz.12194>
59. Fitz, N. F., Wolfe, C. M., Playso, B. E., Biedrzycki, R. J., Lu, Y., Nam, K. N., *et al* (2020) Trem2 deficiency differentially affects phenotype and transcriptome of human APOE3 and APOE4 mice. *Mol. Neurodegener.* **15**, 41
60. Li, Z., Del-Aguila, J. L., Dube, U., Budde, J., Martinez, R., Black, K., *et al* (2018) Genetic variants associated with Alzheimer's disease confer different cerebral cortex cell-type population structure. *Genome Med.* **10**, 43
61. Pfrieger, F. W. (2021) Neurodegenerative diseases and cholesterol: seeing the field through the players. *Front. Aging Neurosci.* **13**, 766587